



*Dedicated to Professor Ionel Haiduc
on the occasion of his 75th anniversary*

COMPARATIVE STUDY OF PHOSPHORUS-CONTAINING POLYMERS WITH HIGH PERFORMANCE PROPERTIES

Diana SERBEZEANU,* Ionela-Daniela CARJA, Tăchiță VLAD-BUBULAC,
Corneliu HAMCIUC and Maria BRUMĂ

“Petru Poni” Institute of Macromolecular Chemistry, Aleea Gr. Ghica Vodă 41A, Iași-700487, Roumania

Received April 27, 2011

Polyesters and poly(ester-imide)s have been synthesized by polycondensation reaction of terephthaloyl bis-(4-oxybenzoyl-chloride) with a mixture of 1,12-dodecanediol and various aromatic bisphenol containing phosphorous taken in different ratios. The chemical structure of the polymers has been confirmed by FT-IR and ¹H NMR spectroscopy. The thermal stability and char yield at high temperature have been evaluated by TGA. The mesomorphic properties have been investigated by differential scanning calorimetry, polarized light microscopy, and X-ray diffraction measurements.

INTRODUCTION

Thermotropic liquid crystalline polymers (TLCPs) represent an important class of high performance materials which combine exceptional properties such as thermal stability, mechanical properties, chemical resistance and melt processability. Aromatic copolyesters represent surely one of the most important class of nematic TLCPs. Our specific interest in aromatic copolyesters containing phosphaphenanthrene bulky groups originates from the attractive properties induced by the presence of this heterocycle containing phosphorus (9,10-dihydro-9-oxa-10-phosphaphenanthrene-10-oxide, **DOPO**): improved solubility, high thermo-oxidative stability, good adhesion, reduced birefringence, flame resistance etc.¹⁻⁵ On the other hand, the utilization of flexible spacers between the calamitic mezoogens is a known solution used to decrease the transition temperatures.⁶

The necessity of new high performance materials based on polymers makes the scientific research more active in order to satisfy important needs: flame retardant and environmentally friendly materials. Flame resistance can be controlled by utilization of flame retardants which improve the resistance to ignition of the materials, and after the fire starts, they act as inhibitors for spreading the flame. Phosphorus-containing compounds have received significant attention for many years because they are considered to be the most effective flame retardants, as demonstrated in recent studies.⁷⁻¹²

Here we present a comparative study on the relationship between the aliphatic/aromatic ratio, polymer liquid crystalline phase structure, flame retardancy, and thermooxidative stability of novel synthesized TLCP aromatic-aliphatic copolyesters and copoly(ester-imide)s based on terephthaloyl bis-(4-oxybenzoyl-chloride) and a mixture of a phosphorus-containing monomer, with an aliphatic diol.

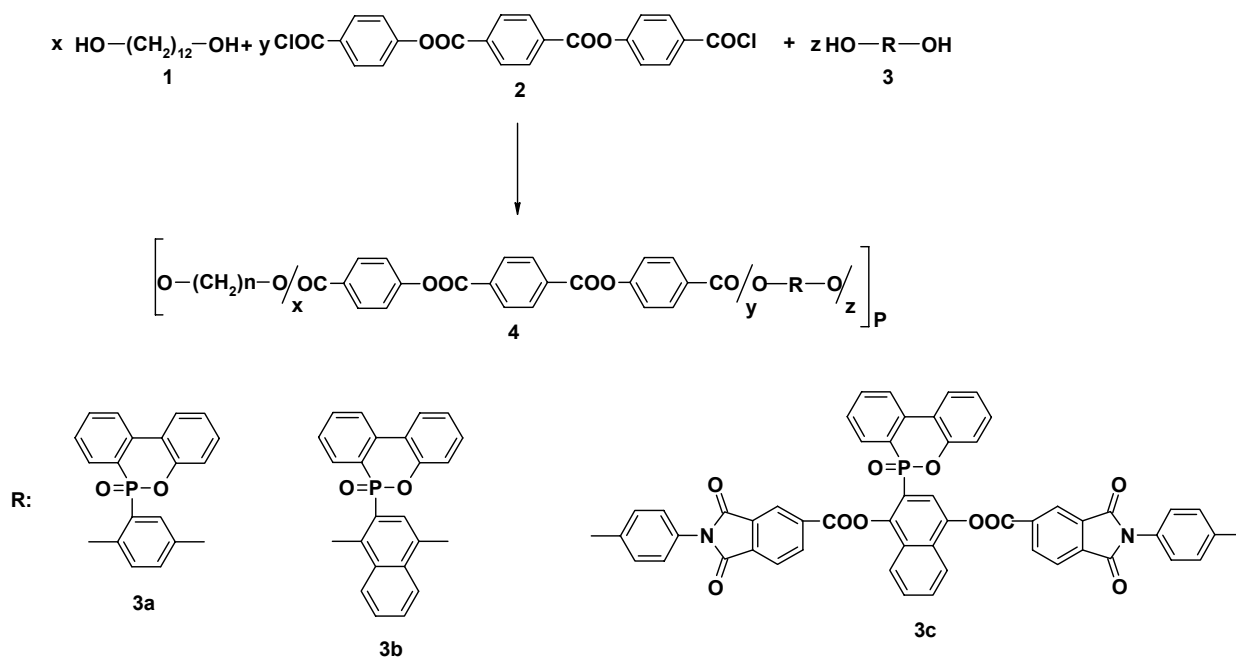
* Corresponding author: diana.serbezeanu@icmpp.ro

RESULTS AND DISCUSSION

The polymers were prepared by solution polycondensation of various molar amounts of aliphatic diol **1**/aromatic bisphenol containing phosphorus **3** with aromatic diacid chloride **2**, by heating the reaction mixture for 20 h at reflux temperature (180 °C) in *o*-dichlorobenzene (Scheme 1). The reaction system was temporarily homogeneous, and then the polymers precipitated during the polycondensation process.

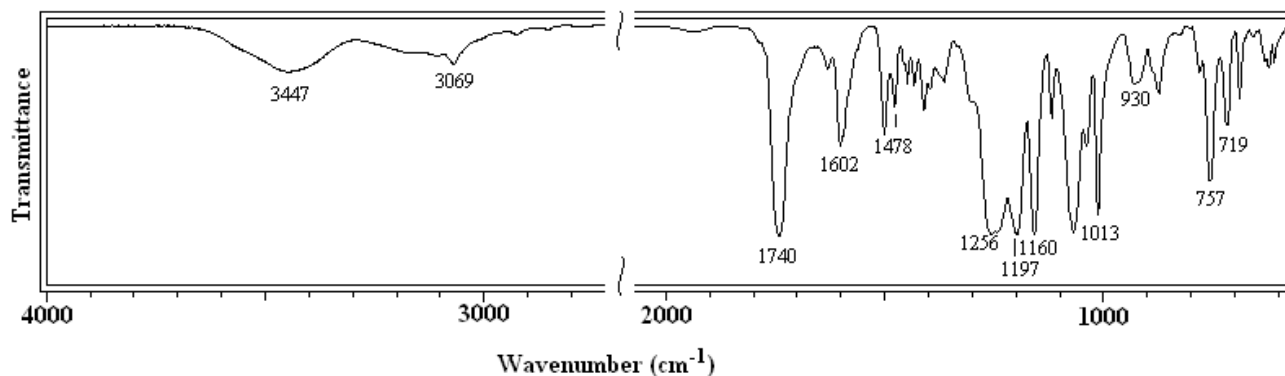
The structure of the polymers **4** was investigated by FT-IR and ¹H NMR spectroscopy. Fig. 1 shows the FT-IR spectrum of polymer **4d**, as an example. As can be seen from the FT-IR spectrum, the most important absorption bands are associated with aromatic C – H (3069 cm⁻¹, stretching vibration), C=O (1740 cm⁻¹, stretching

vibration), ester C – O – C (1256 cm⁻¹ and 1013 cm⁻¹, asymmetric and symmetric stretching vibrations), P – O – Ar (930 cm⁻¹ and 1160 cm⁻¹, stretching vibrations), P – Ar (1478 cm⁻¹), P=O (1197 cm⁻¹), aromatic C – H (757 cm⁻¹, deformation vibration caused by the 1,2-disubstituted aromatic **DOPO** rings), aromatic C – H (719 cm⁻¹, deformation vibration from aromatic terephthaloyl ring) signals. Aromatic C=C bands were found at 1602 cm⁻¹ and 1500 cm⁻¹. The ¹H NMR spectrum of the polymer **4b** exhibited characteristic peaks in the region of 8.38 – 6.87 ppm due to the presence of the aromatic protons. The peaks that characterize the methylene groups closed to the ester unit appeared at 4.5 ppm (O – CH₂, 4H), 1.7 ppm (O – CH₂ – CH₂, 4H) and the peak characterizing the other methylene groups of the structural unit (CH₂, 16H) appeared in the region of δ = 1.49 – 1.34 ppm.



	x	y	z	R
4a	0	1	1	3a
4b	0.5	1	0.5	3a
4c	1	1	0	3a
4d	0	1	1	3b
4e	0.95	1	0.05	3b
4f	0	1	1	3c
4g	0.5	1	0.5	3c
4h	0.95	1	0.05	3c

Scheme 1 – Synthesis of the polymers **4**.

Fig. 1 – FT-IR spectrum of polymer **4d**.

The solubility of the polymers **4** was tested in various solvents, by using 15 mg polymer / mL solvent, at room temperature. All the polymers **4** were easily soluble in DMAc, in NMP and DMSO after heating the solutions, while in solvents such as DMF or CHCl_3 they were only partially soluble. It was expected that the presence of bulky phosphorus-containing units would provide high solubility to these polymers. However, due to high rigidity of the segment coming from the diacid chloride which contains three *p*-phenylene groups connected by ester units, these polymers are only soluble in highly polar solvents.

Thermal stability of the polymers **4**

The thermooxidative stability of the polymers was evaluated by TGA in air at heating rate of 10 °C/min. The most important TGA data (the initial decomposition temperature, temperature of DTG peaks, the yields of char residue at 700 °C) are presented in Table 1. TGA revealed that the polymers were stable up to 350 °C showing a 5%

weight loss in the range of 355 – 408 °C and a 10% weight loss in the range of 385 – 432 °C. From the differential thermogravimetric curves (DTG), it was observed that the polymers decomposed in two-stage weight loss process. The first maximum of decomposition (T_{max1}) was in the range of 400 – 479 °C and was due to the decomposition of ester units and aliphatic moieties which were more sensitive to degradation. The second maximum of the decomposition (T_{max2}) was in the range of 560 – 659 °C and it was due to the degradation of aromatic polymer chain itself (Table 1). The char yield at 700 °C was in the range of 5.6 – 41 % increasing with the content of phosphorus-containing bisphenol **3**. Therefore, the efficiency against the heat transfer and air access from the surface to the inner substrates of the polymeric residue, and the better inhibition of the effectively flame spread can be controlled by increasing the content of phosphorus-containing monomer into the final polymeric matrix.

Table 1

TG and DTG data of samples under study

Polymer	IDT ^a (°C)	T ₁₀ ^b (°C)	T _{max1} ^c (°C)	T _{max2} ^d (°C)	Char Yield at 700 °C (%)
4a	408	432	479	628	41
4b	387	401	421	601	8.4
4c	370	385	410	590	12
4d	385	403	436	659	16
4e	360	389	415	560	5.6
4f	355	390	425	615	33.6
4g	375	400	420	620	27.6
4h	375	385	400	585	18.4

^a Initial decomposition temperature = temperature of 5% weight loss; ^b Temperature of 10% weight loss; ^c First maximum polymer decomposition temperature; ^d Second maximum polymer decomposition temperature.

Thermal transitions of polymers 4

The phase transition temperatures of the polymers **4**, obtained during the first heating, are determined by differential scanning calorimetry (DSC) and the data are summarized in Table 2. The data reveal a considerable effect of molecular structure on the melting temperatures and mesomorphic properties as will be discussed in this section. The polymers **4a**, **4d**, **4f** and **4g** that have no or small aliphatic content exhibit enantiotropic mesophases and reveal nematic phases (*N*, fine textures and schlieren textures), whereas the copolyesters **4e** and **4h** with a higher content of long aliphatic segment as spacer show enantiotropic mesophase and reveal smectic phases (*SmA*, fan-shape texture) because of increasing molecular interaction of the macromolecules. As shown in Table 2, the introduction of laterally attached **DOPO** bulky groups, in small amounts, did not affect the liquid crystalline properties, but with increasing the content of the aromatic diol containing **DOPO** groups the ability of the polymers **4a**, **4d**, **4f** and **4g** to form more ordered liquid crystalline phases decreased. The results suggest that the sterically hindered **DOPO** group might decrease the molecular interaction between macromolecules, which leads to appearance of less ordered liquid crystalline mesophases. The liquid crystalline phases were confirmed by X-ray diffraction experiments and were also compared with the polarized light microscopy (PLM) observations.

Texture analysis

Polarizing light microscopy (PLM) was used to identify the liquid crystalline phases and to complement the phase transitions observed by DSC. Optical micrographs of different textures are shown in Fig. 2. The data of the mesomorphic transition temperatures (K → LC → I) are given in Table 2. A suitable amount of sample for each polymer was charged between two clean glass plates. The samples were heated up to clearing

point which is considered as the liquid crystalline to isotropic state transition (*T_i*). The transition temperatures from crystal to liquid crystalline melt were in the range of 191 °C – 385 °C and depend slightly on the aliphatic content, polymer **4a** having the highest value for the transition K → LC (385 °C). The LC → I transition temperature was in the range of 238 °C – >400 °C and greatly depends on the content of aliphatic diol **1**. Isotropization temperatures increased by decreasing the content of 1,12-dodecanediol. Thus, for the polymers **4a**, **4f** and **4g**, this transition could not be found in PLM investigation because these polymers had too high *T_i* to match the limiting temperature (400 °C) of the hot stage of PLM equipment. *T_i* greatly depends on the content of phosphorous-containing bisphenol **3**.

Upon heating, all as-synthesized polymers **4** formed fine textures (Fig. 2a), difficult to ascribe to a smectic or nematic phase, but similar to those reported for other thermotropic polymers based on terephthaloyl-bis(4-oxyphenylene carbonyl) units.¹³⁻¹⁵ Upon cooling from the isotropic state the polymers **4** behave differently as a function of the structural unit. The flexible methylene spacer groups separate the mesogenic alignment, thereby reducing the overall rigidity. Thus, the polymers containing a higher ratio of 1,12-dodecanediol seems to form textures typical of smectic phases, while the polymers with a smaller content of methylene groups in the structural unit loose the ability to organize into more ordered phases and display only fine threaded textures, typical of nematic phases. For example, in the case of the polymer **4h** upon cooling, some tiny birefringent droplets start to appear from the isotropic state; on continued cooling, these tiny droplets organize in some Schlieren droplets or they grow and populate the whole microscopic view, more ordered phase showing a fan-shaped texture, suggestive of a smectic A phase (Fig. 2b).

Table 2

Phase transition temperatures of polymers 4

Polymer	Transition temperature in °C, from DSC ^{a)}	Transition temperatures in °C, from PLM ^{b)}
4a	K261LC*(-)I	K385LC(-)I
4b	K ₁ 162K ₂ 188LC*(-)I	K246LC310I
4c	K ₁ 158K ₂ 169(188)LC*(-)I	K191LC238I
4d	K268LC*320I	K259LC363I
4e	K ₁ 144K ₂ 181(195)Sm225N(-)I	K202LC299I
4f	K293N(-)I	K308LC>400I

Table 2 (continued)

4g	K ₁ 177K ₂ 186(189)N(-)I	K259LC>400I
4h	K ₁ 167(178)K ₂ 196(204)Sm(238)N304I	K209LC312I

^{a)} Peak temperatures from DSC were taken as the phase transition temperature; ^{b)} Phase transition temperature taken from PLM observation, first heating cycle at a heating rate of 10°C/min; K, K1, K2 – solids, Sm – smectic phase, N – nematic phase, I – isotropic phase, LC, LC* - liquid crystalline phases; (-) Peak temperature not observed by DSC

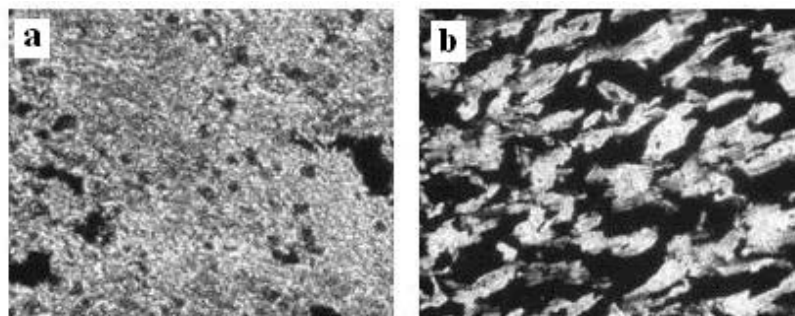


Fig. 2 – Optical micrographs of polymers **4**: (a) polymer **4h** heating cycle at 292°C, fine texture and (b) polymer **4h** cooling cycle at 252°C showing a fan-shaped texture (*SmA* phase).

X-Ray diffraction studies

The mesophase of the polymers was also characterized through X-ray diffraction measurements. The XRD data (percentage crystallinity, *d*-spacing values and Bragg angles) of the polymers **4**, obtained at room temperature, are summarized in Table 3. At room temperature the polymer **4d** showed diffraction peaks only in the wide-angle region. Thus, the scattering halos at around $2\theta = 23.5^\circ$ (*d*-spacing of $\sim 3.8 \text{ \AA}$) revealed a typical semicrystalline behavior. The percent crystallinity of the polymers was determined by bisecting the experimental plot into the crystalline domain and amorphous domain by curve fitting.

The areas under the crystalline and amorphous domain was determined computationally and the percentage crystallinity was calculated. The percentage crystallinity varies from 13.3 % to 43 % depending upon the aliphatic segment content in the polymer. The percentage crystallinity decreased by increasing the content of aromatic diol, from 43 %, in the case of copolyester **4h**, to 13.3 %, for the polyester **4d** without aliphatic diol in the structural unit of the macromolecular chain illustrating repressed crystallization capacities and deregulated molecular packing due to the presence of bulky lateral **DOPO** groups.

Table 3

X-ray diffraction data for the polymers 4			
Polymer	Peak (2 θ)	<i>d</i> -Spacing	Crystallinity
	($^\circ$)	(\AA)	%
4a	19,3	4,6	26
	23,8	3,7	
4b	2,5	35,8	27
	3,4	26,3	
	19	4,6	
	23,4	3,8	
4d	19.8	4.5	13.3
	23.5	3.8	
4f	19.9	4.4	39
	23.0	3.9	

Table 3 (continued)

4g	3.5	24.9	28
	19.6	4.5	
	23.3	3.8	
4h	2.2	39.8	43
	19.4	4.6	
	23.4	3.8	

EXPERIMENTAL

Materials

9, 10-Dihydro-9-oxa-10-phosphaphenanthrene-10-oxide (**DOPO**) was purchased from Chemos GmbH, Germany. Naphthoquinone (**NQ**), trimellitic anhydride chloride (**TMAC**), *p*-aminophenol, terephthalic acid, 4-hydroxybenzoic acid, monomer **1** (1,12-dodecanediol) were provided from Aldrich and used as received. All other reagents were used as received from commercial sources or were purified by standard methods.

Synthesis of the monomers

Terephthaloyl-bis-(4-oxybenzoyl-chloride) **2**, was synthesized by treating the corresponding dicarboxylic acid resulted from the reaction between 4-hydroxybenzoic acid (2 mol) and terephthaloyl chloride (1 mol), with excess thionyl chloride, at reflux temperature, according to a method presented in the literature.⁶ m.p.: 223–226 °C. FT – IR (KBr, cm⁻¹): 1780 (COCl), 1730 (COO), 1600 (C – C aromatic), 1210 (Ph – O – OC).

2-(6-Oxido-6H-dibenz<c,e><1,2>oxaphosphorin-6-yl)-1,4-benzenediol, **3a**, and 2-(6-oxido-6H-dibenz<c,e><1,2>oxaphosphorin-6-yl)-1,4-naphthalenediol, **3b**, were synthesized from **DOPO** and benzoquinone or naphthoquinone, respectively, as described in the literature.^{16,17}

1,4-Bis[N-(4-hydroxyphenyl)phthalimidyl-5-carboxylate]-2-(6-oxido-6H-dibenz<c,e><1,2>oxaphosphorin-6-yl)-naphthalene **3c**, was synthesized from 4-aminophenol and 1,4-[2-(6-oxido-6H-dibenz<c,e><1,2>oxaphosphorin-6-yl)]-naphthalene-bis (trimellitate)dianhydride as previously reported by us.¹⁸ Yield= 80%. FT-IR (KBr, cm⁻¹): 3450 (–OH), 3065 (C – H aromatic), 1780 (C=O, imide carbonyl asymmetric stretching), 1730 (C=O, ester carbonyl and imide carbonyl symmetric stretching), 1600 (C – C aromatic), 1478 (P – Ph), 1368 (C – N – C), 1245 (ester C – O), 1205 (P=O), 1160, 925 (P – O – Ph). ¹H NMR (DMSO-*d*₆, ppm): δ = 9.8 (2H, d), 8.69 (2H,d), 8.45 (2H,m), 8.23 (2H,m), 7.95 (6H,m), 7.62 (4H,m), 7.49 (1H,m), 7.29 (5H,m), 7.09 (1H,d), 6.97 (4H,d). ³¹P NMR (DMSO-*d*₆, ppm): δ= 18.7–16.9.

Synthesis of the polymers

The polymers **4** were prepared by solution polycondensation reaction of the diacid chloride, **2**, namely terephthaloyl-bis(4-oxybenzoyl-chloride), with a mixture of different aromatic phenols containing phosphorus, **3**, and 1,12-dodecanediol.¹⁸⁻²⁰

Measurements

Melting points of the monomers and intermediates were measured on a Melt-Temp II (Laboratory Devices). Fourier transform infrared (FT-IR) spectroscopy was performed on a Bruker Vertex 70 at frequencies ranging from 400 to 4000 cm⁻¹. Samples were mixed with KBr and pressed into pellets. ¹H NMR (400 MHz) spectra were obtained on a Bruker Avance DRX 400 spectrometer. The polymer samples were dissolved in DMSO upon heating and then measured at room temperature. Thermogravimetric analysis (TGA) was performed on 15 mg samples under air atmosphere at a heating rate of 10 °C min⁻¹ using a Mettler Toledo model TGA/SDTA 851 instrument. The differential scanning calorimetry (DSC) analysis was carried out using a Perkin-Elmer Pyris Diamond instrument using nitrogen as a carrier gas at a flow rate of 10 mL/min. The samples were first heated from room temperature to 350 °C using a heating rate of 10 °C/min, then cooled to 20 °C at a cooling rate of 10 °C/min. The melting temperatures (*T*_{m1} and *T*_{m2}) and the liquid crystalline phase transition temperatures of polymers were taken as maximum of endothermic peaks. Polarized light microscopy (PLM) was carried out with an Olympus BH-2 polarized light microscope fitted with a THMS 600/HSF91 hot stage, at a magnification of 200× or 400×. The mesomorphic transition temperature and disappearance of birefringence, that is, the crystal-to-nematic (*T*_m) and nematic-to-isotropic (*T*_i) transition, were noted. The wide-angle X-ray diffraction (WAXD) experiments at room temperature and variable temperature XRD were performed on a D8 Advance Bruker AXS diffractometer using a CuKα source with an emission current of 36 mA and a voltage of 30 kV. Scans were collected over the 2θ = 2 – 40 range using a step size of 0.01° and a count time of 0.5 s/step.

CONCLUSIONS

A series of main chain thermotropic phosphorous-containing polyesters and poly(ester-imide)s was synthesized and studied. The char yield at high temperatures increased by increasing the amount of phosphorus-containing monomers. The thermal transitions and thermotropic liquid crystalline properties were confirmed by DSC and X-ray diffraction experiments and were also compared with the PLM observations. It has been

found that the transition temperatures decrease by increasing the content of aliphatic segment.

Acknowledgements: This work was supported by CNCISIS – UEFISCSU, project number PNII – RU 657/2010.

REFERENCES

1. G. S. Liou and S. H. Hsiao, *J. Polym. Sci. Part A: Polym. Chem.*, **2002**, *40*, 459-470.
2. S. V. Levchik and E. D. Weil, *Polym. Int.*, **2005**, *54*, 11-35.
3. C. S. Zhao, L. Chen and Y. Z. Wang, *J. Polym. Sci. Part A: Polym. Chem.*, **2008**, *46*, 5752-5759.
4. C. Hamciuc, T. Vlad-Bubulac, O. Petreus and G. Lisa, *Polym. Bull.*, **2008**, *60*, 657-664.
5. A. I. Balabanovich, D. Pospiech, A. Korwitz, L. Hausler and C. Harmish, *Polym. Degrad. Stab.*, **2009**, *94*, 355-364.
6. T. Vlad-Bubulac and C. Hamciuc, *Polymer*, **2009**, *50*, 2220-2227.
7. C. S. Wang, C. H. Lin and C. Y. Chen, *J. Polym. Sci. Part A: Polym. Chem.*, **1998**, *36*, 3051-3061.
8. S. Senthil and P. Kannan, *J. Polym. Sci. Part A: Polym. Chem.*, **2001**, *39*, 2396-2403.
9. Y. L. Liu, C. S. Wu, K. Y. Hsu and T. C. Chang, *J. Polym. Sci. Part A: Polym. Chem.*, **2002**, *40*, 2329-2339.
10. X. H. Du, Y. Z. Wang and X. T. Chen, *Polym. Degrad. Stab.*, **2005**, *88*, 52-56.
11. J. Canadell, A. Mantecon and V. Cadiz, *J. Polym. Sci. Part A: Polym. Chem.*, **2007**, *45*, 1980-1992.
12. X. Wang, Y. Hu, L. Song, W. Xing, H. Lu, P. Lv and G. Jie, *Polymer*, **2010**, *51*, 2435-2445.
13. M. H. B. Skovby, R. Lessel and J. Kops, *J. Polym. Sci. Part A: Polym. Chem.*, **1990**, *28*, 75-87.
14. F. Ignatious, R. W. Lenz and S. W. Kantor, *Macromolecules*, **1994**, *27*, 5248-5257.
15. T. F. McCarthy, R. W. Lenz and S. W. Kantor, *Macromolecules*, **1997**, *30*, 2825-2838.
16. Y. S. Sun and C. S. Wang, *Polymer*, **2001**, *42*, 1035-1045.
17. L. Ding, F. E. Karasz, Y. Lin, Y. Pang and L. Liao, *Macromolecules*, **2003**, *36*, 7301-7307.
18. D. Serbezeanu, T. Vlad-Bubulac, C. Hamciuc and M. Aflori, *J. Polym. Sci. Part A: Polym. Chem.*, **2010**, *48*, 5391-5403.
19. D. Serbezeanu, T. Vlad-Bubulac, C. Hamciuc and M. Aflori, *Macromol. Chem. Phys.*, **2010**, *211*, 1460-1471.
20. D. Serbezeanu, T. Vlad-Bubulac, C. Hamciuc, M. Aflori and M. Brumă, *Mater. Plast.*, **2011**, *48*, 117-122.

